EFFECTS OF TiO_2 ADDITIVE ON ELECTROCHEMICAL HYDROGEN STORAGE PROPERTIES OF NANOCRYSTALLINE /AMORPHOUS Mg_2Ni INTERMETALLIC ALLOY

A. Shahcheraghi, F. Dehghani, K. Raeissi*, A. Saatchi and M. H. Enayati

* *k_raeissi@cc.iut.ac.ir*

Received: July 2012 **Accepted: January 2013**

Department of Materials Engineering, Isfahan University of Technology, Isfahan, Iran.

Abstract: *Mg_2Ni alloy and Mg_2Ni–x wt% TiO_2 (x = 3, 5 and 10 wt %) composites are prepared by mechanical alloying. The produced alloy and composites are characterized as the particles with nanocrystalline/amorphous structure. The effects of TiO_2 on hydrogen storage properties are investigated using anodic polarization and electrochemical impedance spectroscopy. It is demonstrated that the initial discharge capacity and exchange current density of hydrogen are increased by adding 5wt% TiO_2, while the cycle stability and bulk hydrogen diffusivity don't change. It is found that the charge transfer resistance of Mg_2Ni–5wt% TiO_2 composite is lower than that of Mg_2Ni alloy. On the other hand, the hydrogen oxidation during the discharge process proceeds more easily on the electrode surface containing TiO_2 additive.*

Keywords: *Magnesium-Nickel alloy; hydrogen storage; mechanical alloying; oxide addition; electrochemical propertiy*

1. INTRODUCTION

Rechargeable alkaline Ni–MH batteries use hydrogen storage alloys as the negative electrode due to their high energy density, great electrochemical properties and non toxicity [1]. Magnesium-based alloys have been studied because of their high hydrogen storage capacity and low cost [2]. However, rapid degradation of capacity in alkaline solutions and slow charge/discharge kinetics prevent their practical applications [3-6]. The attempts have been focusing on improving the electrochemical properties of Mg-based alloys in alkaline solutions [7,8].

In spite of techniqes such as casting and powder metallurgy, promotion of appropriate nano/amorphous structures and defects makes the mechanical alloying (MA) as an exclusive method to modify the structure and surface characteristics of materials used in negative electrodes [7,9]. Numerous works show that the MA improves charge/discharge kinetics by reducing the grain size to nanoscale dimension, which consequently increases the specific surface area. It creates many defects including fine cracks on the surface, which are highly permeable to hydrogen and thus facilitates the activation of powders [10-15].

Some transition metal oxides could be used as catalysts to improve the hydriding/dehydriding kinetics of nanocrystalline Mg-based materials [16,17]. The electrochemical performance of nanocrystalline $LaMg_{12}$-Ni composite produced by MA method was modified significantly with a small amount of TiO_2 and Fe_3O_4 additives [18]. Cui and Luo [19] studied the electrochemical performance of Mg_2Ni-type hydrogen storage alloys and found that the discharge capacity and discharge rate of these alloys were greatly improved with metal oxides addition such as RuO_2 and V_2O_5.

The surface modification obtained by milling Mg-based alloy with an additive has been adopted to improve the electrochemical cycle stability of alloys [20]. Wang et al. [21] reported that the cycle stability of La_2Mg_{17} + 200 wt% Ni composite was improved by mixing of 1wt% Bi_2O_3 through ball-milling.

In this work, the effects of TiO_2 on the electrochemical hydrogen storage properties and charge/discharge kinetic behavior of nanocrystalline /amorphous Mg_2Ni alloy produced by MA were investigated.

2. MATERIAL AND METHODS

Mg_2Ni alloy was prepared through MA. The metal powders of Mg and Ni elements were obtained from Merck and mixed in a planetary ball-mill at stoichiometric ratio of 2:1 for 50 h, under an argon protective atmosphere. The rotational speed during the ball milling was 500 rpm and the ball-to-powder weight ratio was 20:1. $Mg_2Ni–xTiO_2$ (x = 3, 5 and 10 wt %) composites were also produced by ball-milling of produced Mg_2Ni and different amounts of TiO_2 powders for 2 h, by similar process described above. The crystalline structure of the produced alloys was characterized by means of X-ray diffractometer (XRD) (model Philips Xpert-MPD). The surface configuration was characterized by using transmission electron microscope (TEM) (model Philips CM120) and scanning electron microscope (SEM) (model Philips XL30).

For preparing the working electrode, 1 g of alloy powders produced (Mg_2Ni or $Mg_2Ni–xTiO_2$) was mixed thoroughly with 5 g Ni powder and then compressed under 500 MPa pressure into tablet of 16 mm diameter and 0.6 mm thickness.

The electrochemical measurements were performed through an open tri-electrode measurement system in 6 M KOH electrolyte at 298˚K. The Pt and Hg/HgO electrodes were served as the counter and reference electrodes, respectively. Before the measurements, the working electrode was activated in 6 M KOH electrolyte for 1 h. The discharge capacitiy was then measured as follows. The working electrode was first charged at 100 mA g^{-1} cathodic current for 9500 s. Then, it waited for 5 min and then discharged by applying 100 mA g^{-1} anodic current until the potential reached to -0.5 V vs. Hg/HgO. In order to measure the cyclic stability, a charge/discharge current of 100 mA g^{-1} was applied for 8 cycles. Electrochemical impedance spectroscopy (EIS) measurements were carried out using voltage amplitude of 10 mV in the frequency range of 100 kHz^{-10} mHz. The anodic polarization curves of the electrodes were also measured with the scan rate of 1 mVs^{-1} from 0-1200 mV vs. open circuit potential at fully-charged state.

3. RESULT AND DISCUSSION

3. 1. Structural Characterization

The surface area and particle size are the most important factors influencing the hydridation characteristic of particles. Ball-milling process produces fine particles with fresh surfaces which increase hydridation rate [10]. Fig. 1 shows XRD patterns of Mg_2Ni alloy and $Mg_2Ni–x$ wt% TiO_2 (x = 3, 5 and 10 wt %) composites. The peaks of Mg_2Ni phase have appeared after 50 h milling and are wide in appearance. This may indicate a nanocrystalline/amorphous structure of Mg_2Ni which is in agreement with the results obtained by Yuan et al. [7]. As is seen in Fig. 1, the XRD pattern has not been changed by introducing TiO_2 particles. The average crystalline sizes calculated by applying Williamson-Hall formula [22] using XRD patterns are around 6 nm for both Mg_2Ni and $Mg_2Ni–x$ wt% TiO_2 specimens. It seems that the crystal size of Mg_2Ni has not been affected by TiO_2 addition.

TEM images of Mg_2Ni particles and 5%wt TiO_2-containing composite particles after 50 h alloying are shown in Figs. 2 and 3. A feature which consists of nanocrystalline grains embedded in an amorphous matrix can be

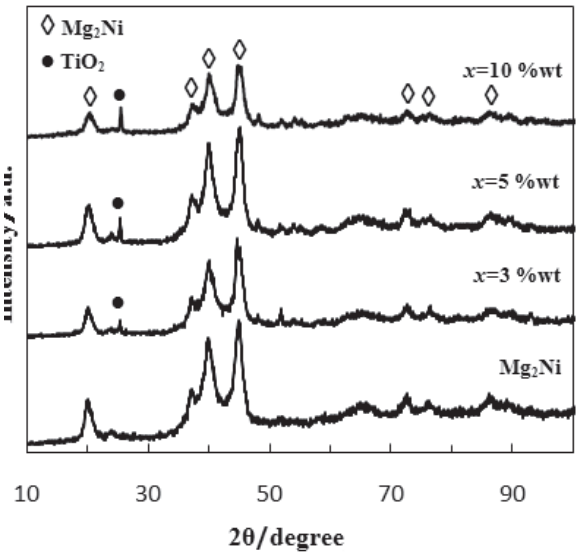

Fig. 1. XRD patterns of Mg_2Ni alloy and $Mg_2Ni–x$ wt% TiO_2 (x = 3, 5 and 10 wt%) composites.

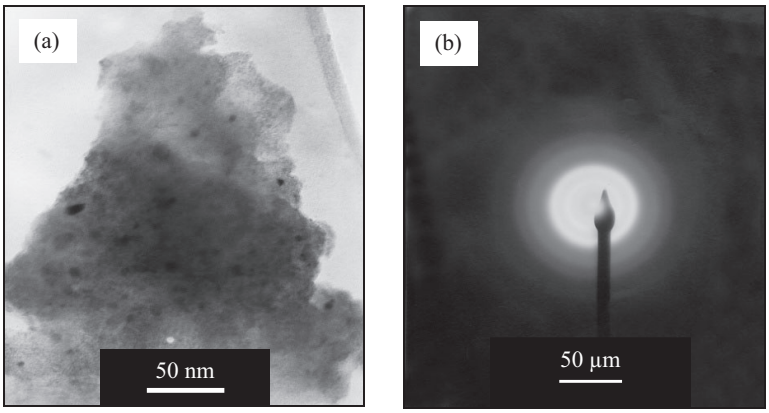

Fig. 2. TEM image of Mg_2Ni alloy: (a) light-field image (b) electron diffraction pattern.

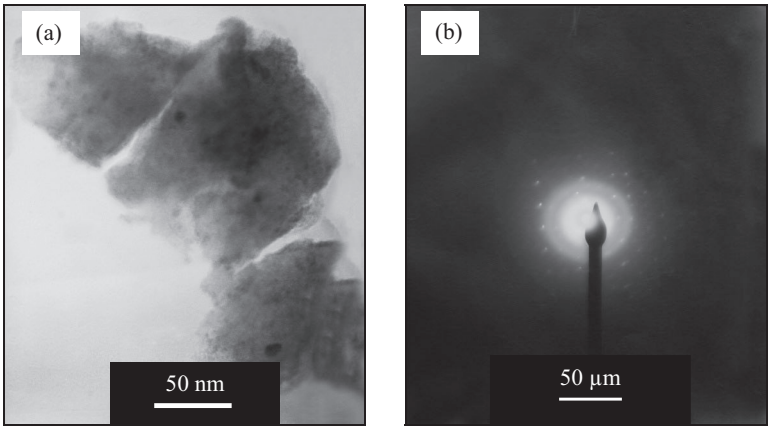

Fig. 3. TEM image of Mg_2Ni–5 wt% TiO_2 composite: (a) light-field image (b) electron diffraction pattern.

recognized on bright-field images of both specimens (Figs. 2a and 3a). As seen in Figs. 2a and 3a, the average grain size is about 10 nm which confirms the results obtained by XRD patterns. The presence of halo rings in electron diffraction (ED) patterns (Figs. 2b and 3b) indicates the existance of amorphous structure [14]. Also, the diffraction rings appeared around the halo confirms the presence of nanocrystalline grains coexisted with the amorphous phase. A very similar results have been obtained for $Mg_{1.8}Ti_{0.2}Ni$ alloy after ball-milling [9] and the melt-spun $Mg_{20-x}La_xNi_{10}$ (x = 2, 4) electrode [23]. On the other hand, The diffracted spots observed on the corresponding ED pattern (Fig. 3b) confirms the presence of micro size particles related to TiO_2.

3. 2. Electrochemical Characteristics

3. 2. 1. Discharge Capacity

Electrochemical galvanostatic charge /discharge curves were used to evaluate the hydrogen discharge capacity. For charging, water break down was peformed in 6 M KOH solution by imposing a 100 mA g^{-1} cathodic current for 9500 s. The atomic hydrogen is absorbed into the interstitial sites of Mg_2Ni alloy and saturates it. After that, a 100 mA g^{-1} anodic current was applied on the hydrogen saturated Mg_2Ni to release the hydrogen. Fig. 4 shows the discharge curves of Mg_2Ni alloy together with Mg_2Ni–x wt% TiO_2 (x = 3, 5 and 10 wt %) composites for the first cycle. The discharge capacity was calculated using the following Eq. (1).

$$Q_{discharge} = It \quad (1)$$

where Q is the discharge capacity (mAh g^{-1}), I is the discharge current density (mA g^{-1}) at cut-off potential (-0.5 V vs. Hg/HgO), and t is the overall discharge time (h). The first-cycle discharge capacities of the samples with 0, 3, 5 and 10 wt% TiO_2 were 62, 27, 80 and 66 mAh g^{-1}, respectively. It is seen that the TiO_2 addition exerts no systematic effect on discharge capacity. The lowest amount of TiO_2 (3 wt%) destroys the discharge capability of the electrode strongly. However, 5 wt% TiO_2 improves the discharge capacity. On the other hand, the highest amount of TiO_2 (i.e. 10 wt%) shows no significant improvement as compared to pure Mg_2Ni alloy. This is in agreement with the results obtained by Wang et al. [18]. They found that althogh 5 wt% TiO_2 increased the discharge capacity of ball-milled nanocrystalline $LaMg_{12}$–Ni alloy, a decresae in discharge capacity was obtained by 3 wt% TiO_2.

3. 2. 2. Cycle Stability

The cycle stability curves of Mg_2Ni alloy and Mg_2Ni–x wt% TiO_2 (x = 5 and 10 wt %) composites are shown in Fig. 5. From these curves, the cycling capacity retention rates expressed by Eq. (2) are calculated after 8 cycles and listed in Table 1.

$$R_n(\%) = (C_n/C_1) \times 100 \quad (2)$$

where C_1 is the discharge capacity at the first cycle and C_n is the discharge capacity at the n-th cycle (n is 8 for current study). As is seen in Fig. 5 and Table 1, no improvement in cyclic performance has been obtained by adding TiO_2 into Mg_2Ni alloy. As reported in previous studies [18-20], the addition of transition metal oxides has not improved the cycle stability of Mg-based alloys.

Cui and Luo [19] reported that the main reason

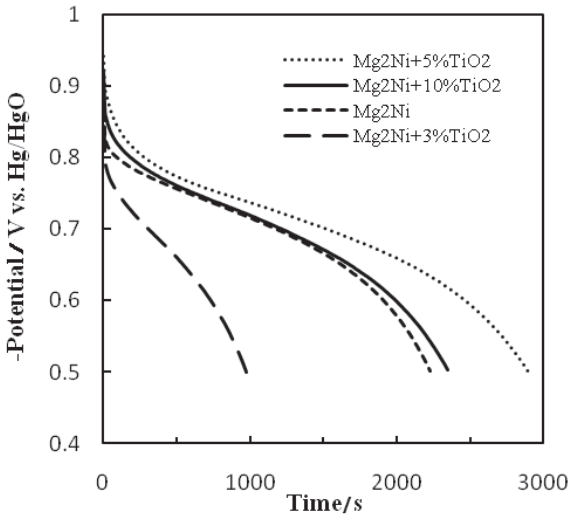

Fig. 4. Discharge curves of the Mg_2Ni alloy and Mg_2Ni–x wt% TiO_2 (x = 3, 5 and 10 wt%) composites for the first cycle.

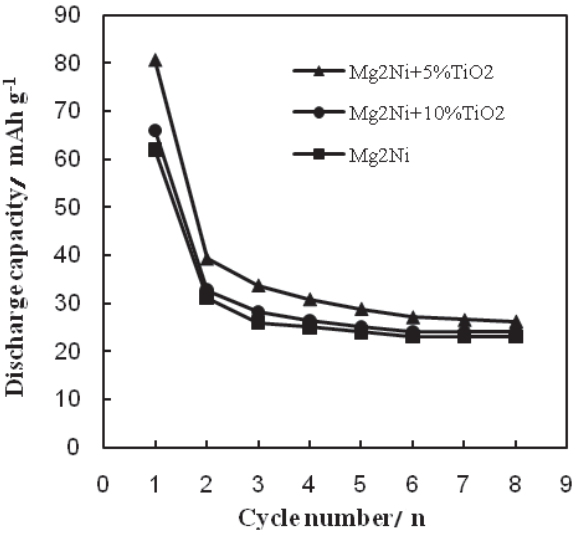

Fig. 5. The cycle stability curves of Mg_2Ni alloy and Mg_2Ni–x wt% TiO_2 (x = 5 and 10 wt%) composites.

Table 1. Maximum discharge capacity (Cmax) and capacity retention rate (R8) of Mg_2Ni alloy and Mg2Ni–x wt% TiO_2 (x = 5 and 10 wt%) composites.

Sample	C_{max} (mAh g^{-1})	R_8 (%)
Mg_2Ni	62	37
Mg_2Ni–5 wt% TiO_2	80	32
Mg_2Ni–10 wt% TiO_2	66	36

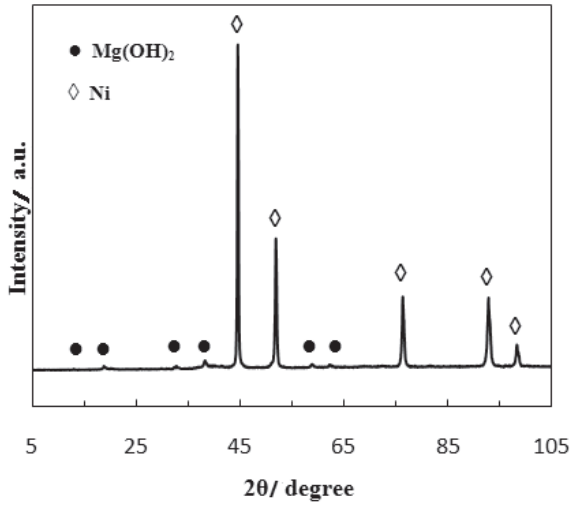

Fig. 6. XRD patterns of the Mg_2Ni alloy after the eighth electrochemical charging/discharging cycle.

for capacity decay of Mg_2Ni-type hydrogen storage material during the charge/discharge cycles is due to the surface oxidation of alloy powder. This layer may inhibit the reduction of hydrogen ions on the surface of electrode and also acts as a diffusion barrier for the hydrogen transport in the bulk of alloy [10]. On the other hand, Wang et al. [18] reported that the degradation of discharge capacity is ascribed to the corrosion of Mg during the cycling in 6 M KOH solution. It seems that TiO_2 addition have no influence on degradation of the electrode during the cycling processes.

XRD pattern of Mg_2Ni alloy taken after the eighth electrochemical charging/discharging cycle is shown in Fig. 6. The peaks of $Mg(OH)_2$ which is due to the oxidation of Mg on surface of the alloy particles, confirm the formation of hydroxide layer on the alloy surface and the subsequent loss of cycle performance. Another factor responsible for the discharge capacity degradation of Mg-based hydride electrodes is the pulverization of this alloy due to the expansion and contraction of cell volume during charge/discharge cycles [24].

Fig. 7 shows SEM images of Mg_2Ni alloy before and after the eighth electrochemical charging/discharging cycle. It is obvious that the smooth surface of alloy particles has changed to a rough one after the eighth cycling indicating the pulverization of electrode.

3. 2. 3. Electrochemical Impedance Spectroscopy (EIS)

Fig. 8 shows the Nyquist plot of Mg_2Ni alloy and Mg_2Ni–5 wt% TiO_2 composite in 6 M KOH solution. The semicircle loop represents the characteristic of charge transfer process at alloy/electrolyte interface which gives rise to the formation of adsorbed hydrogen and hydroxide ions at the interface according to Eq. (3). On the other hand, the straight line at low frequencies with an angle near 45° against the real axis represents Warburg diffusion behavior. The Warburg behavior is due to the difficulties for hydrogen diffusion in the bulk of alloy as represented by Eq. (4). Therefore, the discharge process of the alloy is controlled by both charge transfer process at the electrode /electrolyte

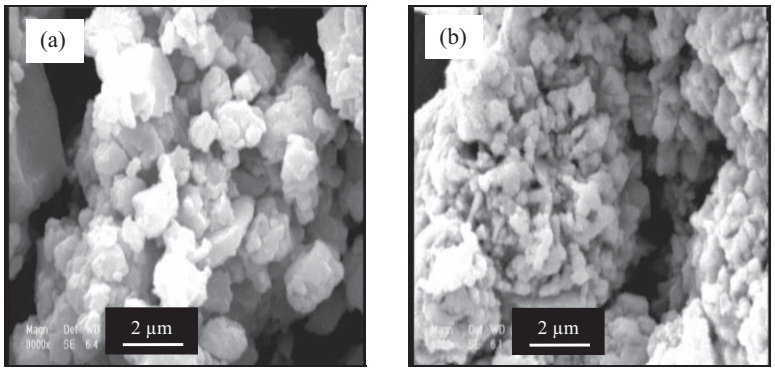

Fig. 7. SEM images of the Mg_2Ni alloy before and after 8 charging/discharging cycles. (a) before cycle; (b) after 8 cycles.

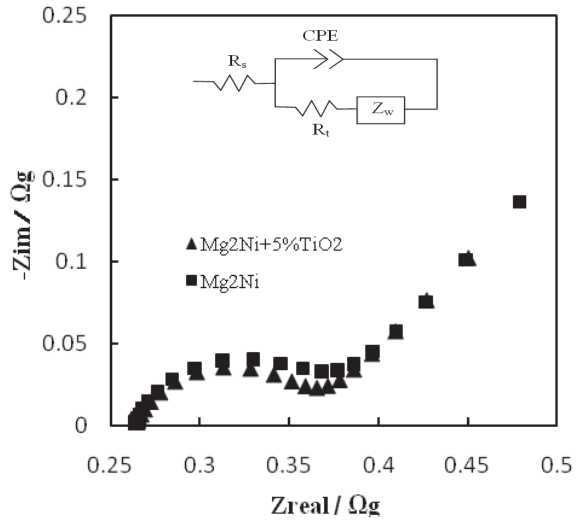

Fig. 8. Electrochemical impedance spectra (Nyquist plot) of the Mg_2Ni alloy and Mg_2Ni–5 wt% TiO_2 composite.

interface and diffusion of hydrogen atom in the alloy at the 0% depth of discharge [25].

$$M + H_2o + e^- \rightleftarrows M - H_{ads} + OH^- \quad (3)$$

$$M - H_{ads} \rightleftarrows MH \quad (4)$$

The electrical equivalent circuit (EC) determined by using the Zview software is shown in Fig. 8. In the EC, R_t is the charge transfer resistance, R_S is the solution resistance, Z_w is the Warburg impedance and CPE is the constant phase element belonging to the high frequency capacitive loops. The Warburg impedance (Z_w) is observed whenever the reaction is under partial or complete mass transport control by diffusion [26]. The term is reserved for the special case of semi-infinite linear diffusion. In the condition of semi-infinite linear diffusion, Z_w for a system at equilibrium can be expressed by [26]:

$$Z_W = \sigma_\omega \omega^{-0.5} - j\sigma_\omega \omega^{-0.5} \quad (5)$$

where σ_ω is the Warburg constant, ω is the ac angular frequency. Z_w can be considered as a series combination of Warburg capacitance (C_w) and a psudoresistance (R_w), which are given by the following equations [26]:

$$C_W = \sigma_W^{-1} \omega^{-0.5} \quad (6)$$

$$R_W = \sigma_\omega \omega^{-0.5} \quad (7)$$

The impedance of CPE is considered as the porosity, roughness and inhomogeneity of the electrode surface and is expressed by the following equation [25]:

$$Z_Q = [Y_o(j\omega)^n]^{-1} \quad (8)$$

where Z_Q is the CPE impedance (Ω cm^{-2}), Y_0 is the CPE admittance (Ω^{-1} sn cm^{-2}). The parameter n is a constant, which shows the degree of deviation from ideal capacitive behavior.

The charge transfer resistance (R_t) and its values derived from proposed EC are given in Fig. 8 and Table 2, respectively. It can be seen that the radius of semicircle for Mg_2Ni–5 wt% TiO_2 composite is smaller than that of Mg_2Ni alloy. Thus, the charge transfer resistance of Mg_2Ni–5 wt% TiO_2 composite is lower than that of Mg_2Ni alloy. The exchange current density (i_0), which is a measure of electrocatalytic nature of the alloy electrode, was calculated by Cui and luo [19] according to Eq. (9).

Table 2. The impedance values and exchange current density (i_0) for the Mg_2Ni alloy and Mg_2Ni–5 wt% TiO_2 composite.

Sample	R_t (Ωg)	CPE-T (F g^{-1})	CPE-P	Z_w-R ($g^{-1}\Omega^{-1}s^{-0.5}$)	Z_w-T ($g^{-1}\Omega^{-1}s^{-0.5}$)	Z_w-P	i_o (mA g^{-1})
Mg_2Ni	0.06	1	0.70	5.3×10^{-8}	5.1×10^{-10}	0.33	214
Mg_2Ni-5% TiO_2	0.05	0.5	0.77	5.3×10^{-8}	$5.\times10^{-10}$	0.30	257

$$i_0 = \frac{RT}{nR_tF} \quad (9)$$

where R is the gas constant, T is the absolute temperature, n is the number of transferred electrons, F is the Faraday constant. Table 2 show that the value of i_0 is increased (43 mA g^{-1}) by adding 5 wt% TiO_2 which indicates higher electrocatalytic nature of the electrode. By adding TiO_2, surface of the alloy powder is covered with fine particles of TiO_2 , and thus, the overpotential is reduced [19]. This accelerates charge transfer on the surface of electrode. Thus, electrocatalytic activity on alloy surface will be improved by the presence of TiO_2. This result is in a good agreement with the maximum discharge capacity obtained for Mg_2Ni–5 wt% TiO_2 composite.

In the Nyquist plot (Fig. 8) at low frequencies, the similar behavior on Warburg diffusion indicates that the diffusion coefficient of hydrogen atoms is unchanged [18] in the presence of TiO_2.

3. 2. 4. Anodic Polarization

Fig. 9 shows the anodic polarization curves of Mg_2Ni alloy and Mg_2Ni–5 wt% TiO_2 composite at fully charged state. Because the hydrogen diffusivity rate is almost the same in the bulk of both electrodes, the anodic peak current can be attributed to the oxidation of absorbed hydrogen according to Eq. (3) [19]. As is seen, the anodic peak current density increases by the presence of TiO_2 indicating that the hydrogen oxidation reaction proceeds more easily on the surface of this electrode. This result is in a good agreement with the maximum discharge capacity obtained for Mg_2Ni–5 wt% TiO_2 composite sample.

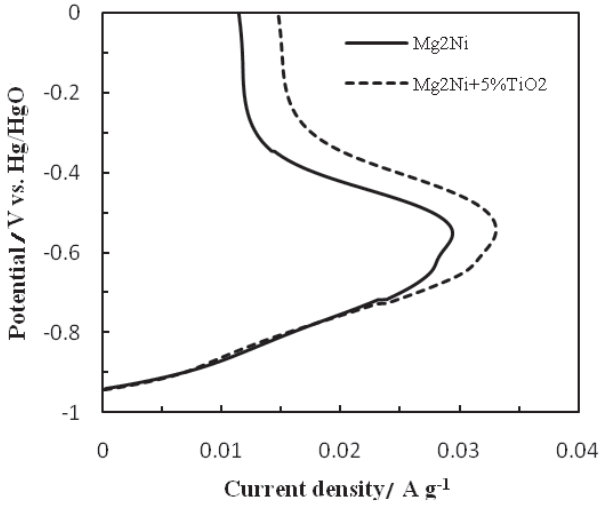

Fig. 9. Anodic polarization curves of the Mg_2Ni alloy and Mg_2Ni–5 wt% TiO_2 composite after full charging.

4. CONCLUSION

Nanocrystalline/amorphous Mg_2Ni alloy was prepared by ball-milling and the effects of TiO_2 additive on the electrochemical hydrogen storage properties were investigated. The initial discharge capacities of the composites with 5 and 10 wt% TiO_2 were larger than that for pure Mg_2Ni alloy. However, no improvement in cyclic performance has been obtained by adding TiO_2. The charge/discharge kinetics of electrodes were studied by using anodic polarization and EIS techniques. It was shown that the exchange current density, i0, which is a measure of electrocatalytic nature of the alloy electrode was greatly increased by adding 5wt%TiO_2. This would be useful in enhancement of the charge/discharge rate. On the other hand, hydrogen diffusivity in the bulk of alloy showed no obvious variation by adding TiO_2.

REFERENCES

1. Xiangdong, L., Lihong, H., Xiao T., Hongwei, F. and Bo, C., "Activation characteristics and microstructure of Mg_2Ni /$Mm_{0.3}Ml_{0.7}Ni_{3.55}Co_{0.75}Mn_{0.4}Al_{0.3}$ composite hydrogen storage alloys prepared by two-step re-melting." Int. J. Hydrogen Energ., 2007, 32, 4939.
2. Jiao, L. F., Yuan, H. T., Wang, Y. J. and Wang, Y. M., "Electrochemical properties of magnesium based hydrogen storage alloys improved by transition metal boride and silicide additives." Int. J. Hydrogen Energ., 2009, 34, 1476.
3. Hsu, F. H., Lin, C. K., Lee, S. L., Lin, C. Y. and Bor, H. Y., "Effect of Mg_3MnNi_2 on the electrochemical characteristics of Mg_2Ni

electrode alloy." J. Power Sources, 2010,195, 374.
4. Kim, J. S., Lee, C. R., Choi, J. W. and Kang, S. G., "Effects of F-treatment on degradation of Mg_2Ni electrode fabricated by mechanical alloying." J. Power Sources, 2002, 104, 201.
5. Ruggeri, S., Roue, L., Huot, J., Schulz, R., Aymard, L. and Tarascon, J.M., "Properties of mechanically alloyed Mg–Ni–Ti ternary hydrogen storage alloys for Ni-MH batteries." J. Power Sources, 2002, 112, 547.
6. Zhang, Y., Jiao, L., Yuan, H., Miao, Y., Wang, Q., Liu, L., Liu, G., Liu, S. and Wang, Y., "Study on the electrochemical properties of MgNi–CuO hydrogen storage composite materials." J. Alloy Compd., 2009, 481, 639.
7. Yuan, H., Li, Q., Song, H., Wang, Y. and Liu, J., "Electrochemical characteristics of Mg_2Ni-type alloys prepared by mechanical alloying." J. Alloy Compd., 2003, 353, 322.
8. Cui, N. and Luo, J. L., "An AC impedance study of self-discharge mechanism of nickel–metal hydride (Ni–MH) battery using Mg_2Ni-type hydrogen storage alloy anode.", Electrochim. Acta, 2000, 45, 3973.
9. Chen, J., Yao, P., Bradhurst, D. H., Dou, S. X. and Liu, H. K., "Mg_2Ni-based hydrogen storage alloys for metal hydride electrodes." J. Alloy Compd., 1999, 293–295, 675.
10. Niu, H., "Electrochemical performance of ball-milled Mg_2Ni electrodes", M. Sc. Thesis, University of Windsor, 1999.
11. Nohara, S., Fujita, N., Zhang, S. G., Inoue, H. and Iwakura, C., "Electrochemical characteristics of a homogeneous amorphous alloy prepared by ball-milling MgNi with Ni.", J. Alloy Compd., 1998, 267, 76.
12. Iwakura, C., Inoue, H., Zhang, S. G. and Nohara, S., "Hydriding and electrochemical characteristics of a homogeneous amorphous Mg_2Ni-Ni composite.", J. Alloy Compd., 1998, 270 142.
13. Cui, N., He, P. and Luo, J. L., "Synthesis and characterization of nanocrystalline magnesium-based hydrogen storage alloy electrode materials." Electrochim. Acta, 1999, 44, 3549.
14. Goo, N. H., Jeong, W. T. and Lee, K. S., "Effects of Zr addition on discharge properties of mechanically alloyed Mg_2Ni hydrogen-storage alloy electrode." J. Power Sources, 2000, 87, 118.
15. Zhang, P., Wei, X., Liu, Y., Zhu, J. and Yu G., "Effects of metal oxides addition on the performance of La1. $3CaMg_{0.7}Ni_9$ hydrogen storage alloy." Int. J. Hydrogen Energ., 2008, 33, 1304.
16. Oelerich, W., Klassen, T. and Bormann R., "Metal oxides as catalysts for improved hydrogen sorption in nanocrystalline Mg-based materials.", J. Alloy Compd., 2001, 315, 237.
17. Gao, R. G., Tu, J. P., Wang, X. L., Zhang, X. B. and Chen, C. P., "The absorption and desorption properties of nanocrystalline $Mg_2Ni_{0.75}$ $Cr_{0.25}$ alloy containing TiO_2 nanoparticles." J. Alloy Compd., 2003, 356-357, 649.
18. Wang, Y., Gao, X. P., Lu, Z. W., Hu, W. K., Zhou, Z., Qu, J. Q. and Shen, P. W., "Effects of metal oxides on electrochemical hydrogen storage of nanocrystalline $LaMg_{12}$–Ni composites." Electrochim. Acta, 2005, 50, 2187.
19. Cui, N. and Luo J. L., "Effects of oxide additions on electrochemical hydriding and dehydriding of behavior Mg_2Ni-type hydrogen storage alloy electrode in 6M KOH solution." Electrochim. Acta, 1998, 44, 711.
20. Rongear, C., Grosjean, M. H., Ruggeri, S., Dehmas, M., Bourlot, S., Marcotte S., and Roue L.,"Evaluation of different approaches for improving the cycle life of MgNi-based electrodes for Ni-MH batterries. " J. Power Sources, 2006, 158, 747.
21. Wang, L., Wang, X. H., Chen, L. X., Chen, C. P., Xiao, X. Z., Gao, L. H. and Wang, Q. D., "Effects of ball-milling time and Bi_2O_3 addition on electrochemical performance of ball-milled La_2Mg_{17} + 200 wt.% Ni composites." J. Alloy Compd., 2006, 416, 194.
22. Cullity, B. D., "Elements of X-ray Diffraction.", 2nd ed., Addison Wesley, london, 1978.
23. Zhang, Y., Li, B., Ren, H., Pang, Z., Guo, S. and Wang, X., "An electrochemical investigation of melt-spun nanocrystalline and amorphous Mg_2Ni-type electrode alloys." J. Alloy Compd., 2009, 477, 759.
24. Huang, H., Huang, K. and Liu, S., "Microstructures and electrochemical properties of Mg0.9Ti0.1Ni1-xMx (M=Co, Mn; x=0, 0.1, 0.2) hydrogen storage alloys.", Powder Technol., 2010, 198, 144.

25. Cui, N. and Luo J. L., "AC impedance studies of the discharge process of a Mg_2Ni-type hydrogen storage alloy electrode in 6 M KOH solution.", J. Alloy Compd., 1998, 265, 305.
26. Khorrami, M. R., Raeissi, K., Shahban, H., Torkan, M. A. and Saatchi, A., "Corrosion behavior of carbon steel in carbon dioxide-loaded activated methyl diethanol amine solution." Corros. Sci., 2008, 64, 124.